Influence of the Aspect Ratio on the Aerodynamics of the Delta Wing at High Angle of Attack

Y. Zohar* and J. Er-El†
Technion—Israel Institute of Technology, Haifa, Israel

The influence of aspect ratio on the contribution of the leading-edge vortices to the loading of the delta wing has been studied experimentally. The study is based on surface pressure measurements of four wings having aspect ratios of 1.07-2.80 (55 ≤ 75 deg sweep angles). Results show that the suction induced by the leading-edge vortices increases with incidence as long as they are not affected by vortex breakdown. In higher-aspect-ratio wings, when vortex breakdown is present on the wing, the vortex-induced suction continues to increase with incidence at a decreasing rate until the breakdown has reached the apex region. In lower-aspect-ratio wings, however, the vortex-induced suction decreases with incidence as the breakdown crosses the trailing edge. The magnitude of the slope of this decrease is smaller in lower-aspect-ratio wings. This may indicate that lower-aspect-ratio delta wings are preferable for future aircraft designed for poststall flight.

Nomenclature

A = wing area
AR = aspect ratio
c = wing root chord
C_L = lift coefficient
C_M = pitching moment coefficient, referred to the wing apex
C_N = normal force coefficient
C_{NP} = potential contribution to C_N
C_{NV} = vortex-induced contribution to C_N
C_p = pressure coefficient $[(p - p_\infty)/q]$
p = pressure
q = dynamic pressure
$s(x)$ = wing local semispan
x = nondimensional chordwise coordinate $(x = x/c)$
y = nondimensional local spanwise coordinate $[y = y/s(x)]$
α = angle of attack
ΔC_{Nvb} = $\Delta C_{Nvb} = (C_{Nmax} - C_{Nvb})/C_{Nmax}$

Superscripts

l = at the lower surface
u = at the upper surface

Subscripts

max = maximum
min = minimum
vb = vortex breakdown appears at the trailing edge
∞ = freestream

Introduction

THE flowfield about a delta wing at moderate and high angles of attack is characterized by shed vortices produced all along the leading edge. These vortices contribute to the lift of the wing by inducing suction on its upper surface. As long as the vortices are not affected by vortex breakdown (VB), the vortex lift increases with incidence angle. When the vortices are affected by breakdown, their contribution to the lift is disrupted.

The effects of the VB phenomenon on the flowfield and on the aerodynamic properties of the delta wing were investigated primarily by experimental means. Analytical or numerical models cannot, at the present time, explain or simulate the flowfield about the wing at high angles of attack when the vortices are affected by VB. Wentz and Kohleman[1] carried out a parametric investigation of the effects of VB on the aerodynamic properties of the delta wing. By means of flow visualization, they determined the chordwise VB position as a function of angle of attack for a series of delta wings with different aspect ratios. In addition, they measured the normal force and pitching moments of these wings. Their results show that the critical angle of attack at which VB appears at the trailing edge is a function of the aspect ratio. Increasing the angle of attack results in an upstream migration of the VB toward the apex. The results of Wentz and Kohleman show that the normal force was affected by VB and that this effect is a function of the VB position and the aspect ratio of the wing.

The effect of VB on the leading-edge vortices is evident in the suction peaks they induce on the upper surface of the wing and can be observed in the wing surface pressure distribution. Pressure measurements on delta wings with vortices affected by VB have been carried out by a number of researchers. The first work was by Lawford and Beauchamp[2] on a 70 deg swept delta wing with four pressure taps. Later works were carried out on models with a considerably larger number of pressure taps. Hummel[3] investigated a delta wing having $AR = 1$ (76 deg sweep). This study was carried out at a constant angle of attack and the variations in the position of VB were achieved by yawing the wing. Kirkpatrick[4] made pressure measurements (using a manometer board) on a 68 deg swept wing for a series of angles of attack. McKernan and Nelson[5] conducted a similar study on a 70 deg swept wing, using a more accurate pressure measurement system. All the aforementioned studies showed that in the incidence angles where the VB is not present on the wing, the suction induced by the leading-edge vortices increased with incidence. When the vortices are affected by VB, the results in Refs. 3 and 5 indicate that, downstream of the VB point, there is a reduction in the rate of change of the peak suction (at a given chordwise station) with incidence angle. The results in Ref. 4 disagree with these observations and indicate a local reduction in the suction underneath the breakdown point and a recovery when the breakdown point moves upstream as the angle of attack increases.

For wings with lower sweep angles, measurements have been carried out by Cheremukin et al.[6] on a 60 deg swept wing.

Received March 4, 1986; revision received June 29, 1987.

*Graduate Student, Department of Aeronautical Engineering; currently at the University of Southern California, Los Angeles.
†Senior Lecturer, Department of Aeronautical Engineering.

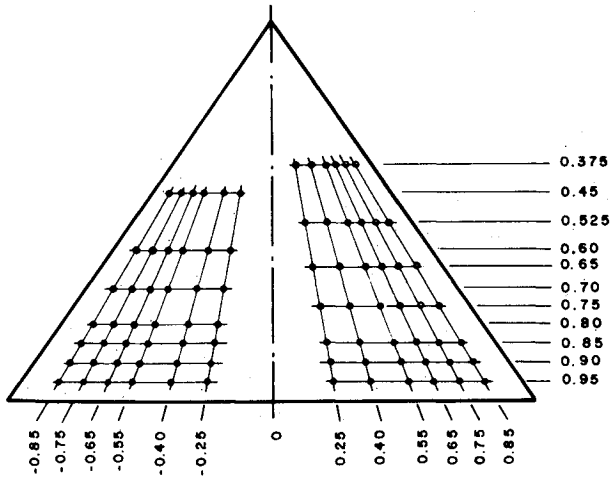

Fig. 1 Map of the pressure holes on the 55 deg swept delta.

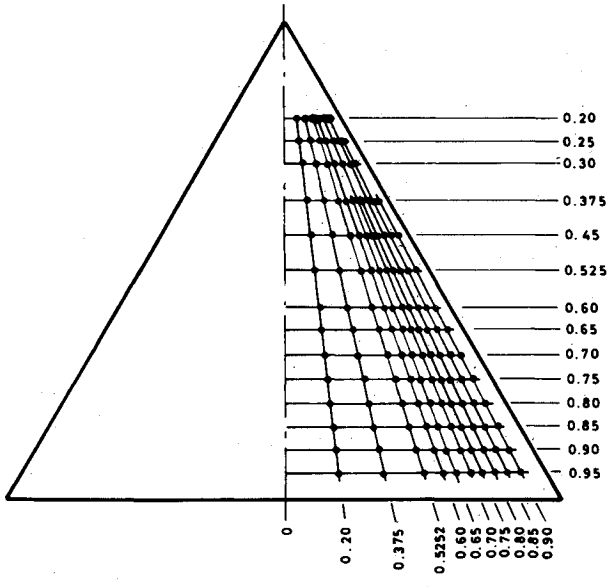

Fig. 2 Map of the pressure holes on the 60 deg swept delta.

Table 1 Geometrical data for the experimental models

Model wing sweep angles, deg	$\mathcal{R}$	CR, mm	t/Cr
55	2.80	239	0.0192
60	2.31	246	0.0187
70	1.46	268	0.0172
74	1.07	302	0.0152

The measurements were made only on the upper surface of the wing at the incidence range in which VB is present on the wing ($\alpha > 15$ deg). No information or reference to the pressure measurement system is given in this paper. It should be noted that the C_L values obtained in this work are at variance with previous results in Refs. 1 and 7.

The objective of this investigation is to study the influence of the aspect ratio on the loading of the delta wing, the contribution of the leading-edge vortices to this loading, and the effect of VB on this contribution. The study is carried out on a series of delta wings having sweep angles of 55–75 deg (aspect ratios of 2.80–1.07). This sweep angle range includes a majority of delta wings in both present and future delta wing aircraft configurations. The study is based on pressure measurements on these wings using the same measurement system, the same wind tunnel, and the same wing holder. The identical conditions at which the tests were conducted reduces the bias that might be introduced by these factors and thus might avoid some of the discrepancies evident in previous data sets.

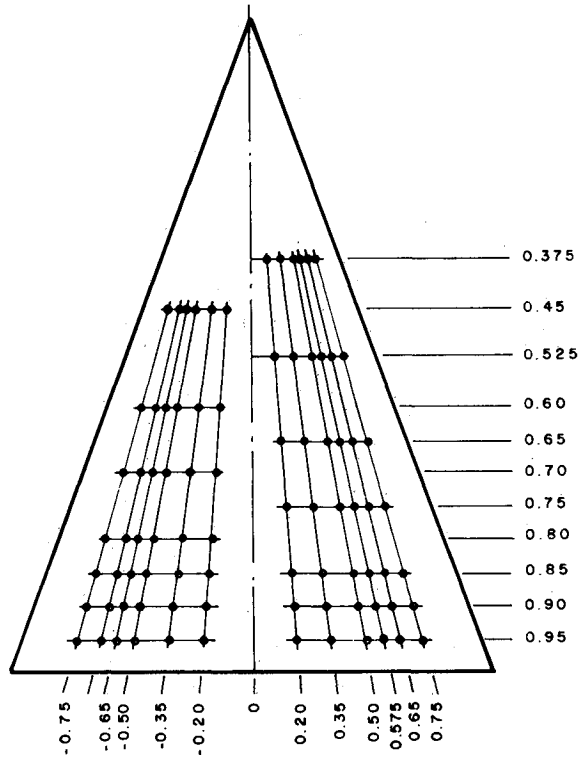

Fig. 3 Map of the pressure holes on the 70 deg swept delta.

Experimental Setup and Procedure

The tests were carried out at the subsonic wind tunnel of the Aeronautical Engineering Department in Technion. The test models consisted of four delta wings having sweep angles of 55, 60, 70 and 75 deg (aspect ratios of 2.80, 2.31, 1.46, and 1.07, respectively). The geometrical data of these models are given in Table 1.

Each of these wings was equipped with approximately 130 pressure measurement ports, concentrated on one of the surfaces. In the 55 and 70 deg swept wings, the pressure holes were arranged on the two sides of the measurement surface of each wing, as depicted in Figs. 1 and 3, whereas in the 60 and 75 deg swept wings, they were arranged on one side only (Figs. 2 and 4). The arrangement of the pressure holes in the latter two wings provided higher spatial resolution for the given number of pressure ports.

The wings are attached to the model-mounting system in the wind tunnel via a wing holder. This holder is constructed as a vertical fin and is attached to the wing on the surface opposite to the pressure measurement surface along its root chord. This setup leaves the pressure measurement surface free of obstructions. The pressure measurement tubes, which emanate from the wing, are attached to this holder in a compact form.

The pressure measurement system is based on three 48 port Scanivalve modules, each connected to a pressure transducer. This system provides the readings of the surface pressures, the freestream dynamic pressure, and a calibration pressure of 10.16 cm (4 in.) water. The calibration pressure was determined by a micromanometer with resolution of ± 0.001 in. water. A detailed description of the experimental setup is given in Ref. 7.

In each experiment, the reading of the calibration pressure was obtained by each of the pressure transducers. An experiment was considered acceptable when the difference

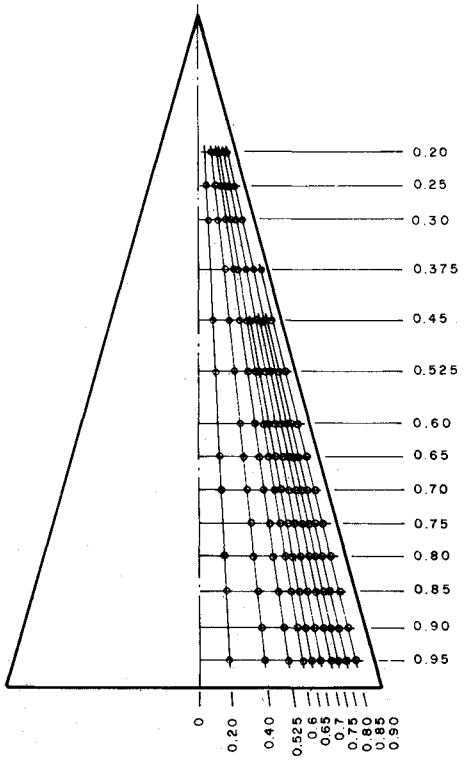

Fig. 4 Map of the pressure holes on the 75 deg swept delta.

between each of these readings and the micromanometer reading did not exceed 1%.

In a typical experiment, the wing was set at a prescribed angle of attack, and the measurements were taken with the pressure measurement surface as the upper surface. The wing was then turned over so that the pressure measurement surface became the lower surface, and the measurements resumed.

Results and Discussion

The measurements were carried out at an airspeed of 32 m/s and at angles of attack ranging from 0 deg to the respective angles at which the VB point has reached the wing apex. A detailed account of the experimental program and the data gathered is given in Ref. 8.

Although the tests were conducted on the four wings, the results and analysis pertaining to the effects of the aspect ratio will be shown, mainly, for two of the four wings tested—the 60 and 75 deg swept delta wings. These two wings illustrate the differences in the vortex lift and VB characteristics of moderate and highly swept wings, respectively.

Pressure Distributions

Figures 5 and 6 feature the spanwise pressure distributions for the 60 deg delta at $\alpha = 15$ deg and the 75 deg delta at $\alpha = 20$ deg. At these angles (at which VB has not affected the suction induced by the vortices), the C_N values of both wings are approximately equal ($C_N = 0.78$). Thus, the contribution of the leading-edge vortices to the loading of the wings can be directly compared.

On the upper surface of each of these wings, the pressure coefficients are characterized by the suction peaks induced by the leading-edge vortices. In both wings, the spanwise $|C_{p,\min}^{u}|$ values in these peaks is largest near the apex and decreases in the downstream direction toward the trailing edge where the Kutta condition prevails. The typical nondimensional width of the vortex-induced suction is larger in the highly swept wing, while $|C_{p,\min}^{u}|$ is smaller. The larger nondimensionalized width in this wing is consistent with analytical predictions[9,10] of high-angle-of-attack aerodynamics of delta wings.

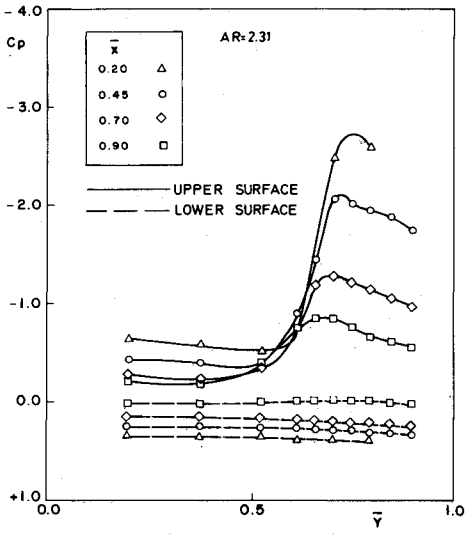

Fig. 5 Spanwise pressure distributions on the 60 deg delta at $\alpha = 15$ deg.

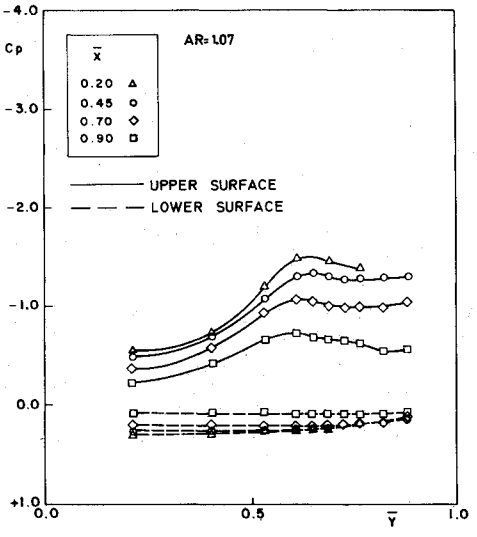

Fig. 6 Spanwise pressure distributions on the 75 deg delta at $\alpha = 20$ deg.

On the lower (windward) surface of each wing, the C_p values are, in general, positive. The spanwise pressure distributions are approximately uniform in the spanwise direction and decrease outwardly toward the leading edge where the pressure on the upper and lower sides of the wing are equal. This indicates that the influence of the leading-edge vortices is, in general, not evident on the lower surface. The C_p^l values, which are largest at the apex, decrease in the downstream direction and may become negative at the trailing-edge region (see, for example, the values of C_p^l along $\bar{y} = 0.7$).

The effect of angle of attack on the two wings is shown in Figs. 7 and 8, which feature the spanwise C_p profiles at $\bar{x} = 0.45$ for a series of incidence angles. The chordwise VB position at these angles are also denoted in the figures. For the 60 deg delta, $|C_{p,\min}^{u}|$ increases with incidence, regardless of VB position as long as it has not reached the apex ($\alpha \leq 32$ deg). At $\alpha > 32$ deg, the suction peaks disappear, indicating that the vortex system no longer exists. For the 75 deg delta, $|C_{p,\min}^{u}|$ increases with incidence up to the incidence angle where VB appears at the trailing edge ($\alpha \cong 35$ deg). At higher incidence angles, $|C_{p,\min}^{u}|$ decreases with increasing incidence, and when VB has reached the apex, the suction peaks disappear in a manner similar to the 60 deg delta.

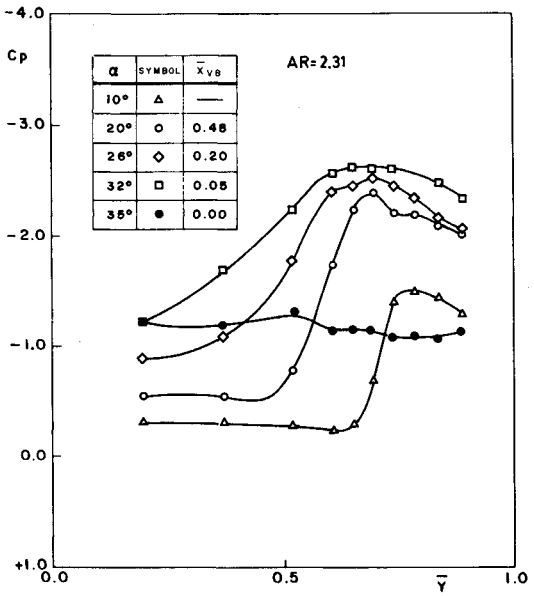

Fig. 7 Spanwise pressure distributions on the 60 deg delta for $\bar{x} = 0.45$ at various incidence angles.

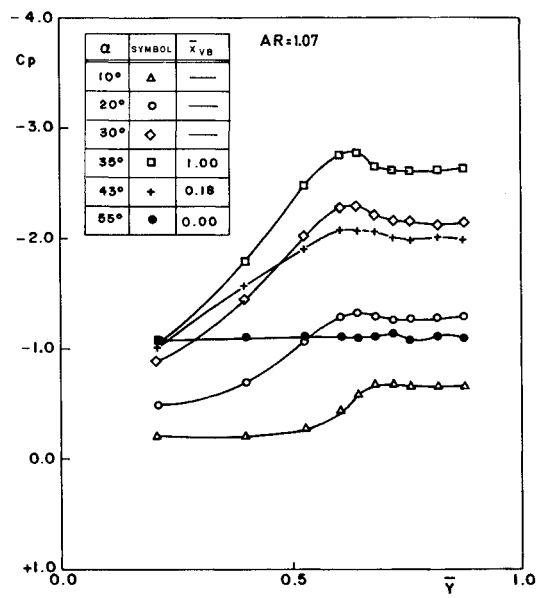

Fig. 8 Spanwise pressure distributions on the 75 deg delta for $\bar{x} = 0.45$ at various incidence angles.

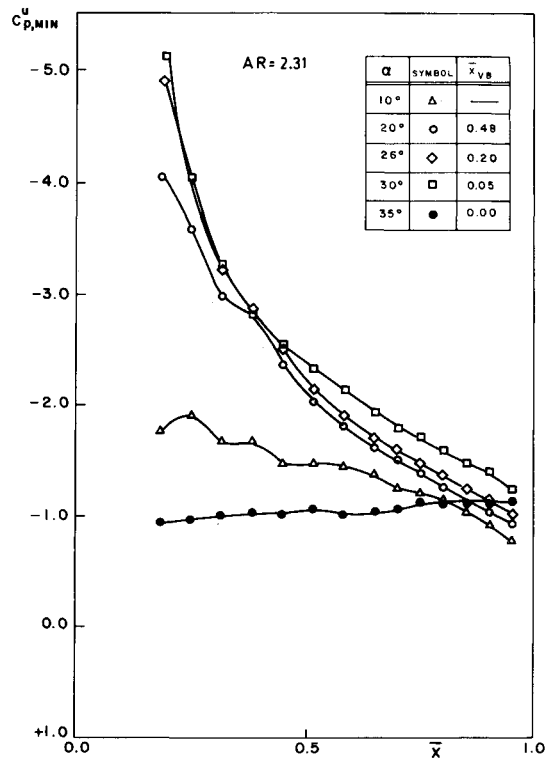

Fig. 9 Chordwise $C^u_{p,\min}$ profiles on the 60 deg delta at various incidence angles.

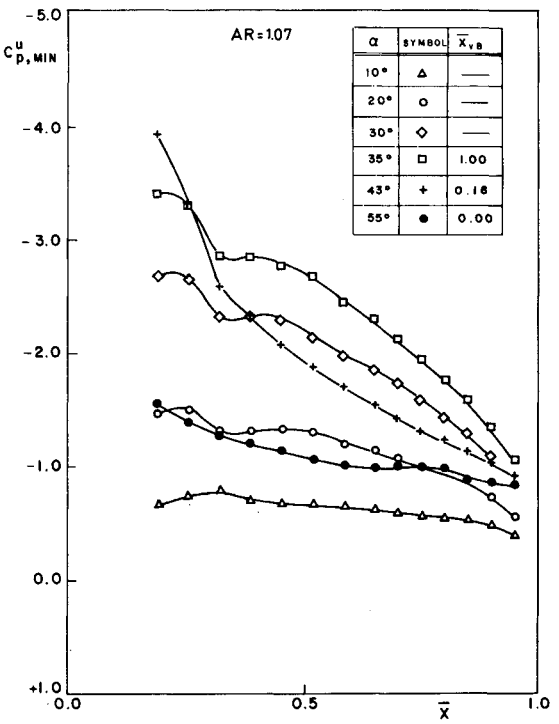

Fig. 10 Chordwise $C^u_{p,\min}$ profiles on the 75 deg delta at various incidence angles.

Figures 9 and 10 feature $|C^u_{p,\min}(\bar{x})|$ at a series of angles of attack for the 60 and 75 deg deltas, respectively. The respective positions of VB at each of these angles are also denoted in these figures. For both wings, $|C^u_{p,\min}(\bar{x})|$ is, in general, largest at the apex region and decreases in the chordwise direction toward the trailing edge, as expected. VB affects the $|C^u_{p,\min}(\bar{x})|$ variation with α differently for each wing. For the 60 deg swept wing (Fig. 9), $\partial|C^u_{p,\min}(x)|/\partial\alpha$ remains positive as long as the VB has not reached the apex. However, its values upstream of the VB are larger than those downstream of it. For the 75 deg swept wing (Fig. 10), the presence of VB, even at the aft section of the wing, causes a decrease in $|C^u_{p,\min}(\bar{x})|$ throughout most of the wing except the apex region. When the VB reaches the apex region, the suction peaks on both wings practically disappear.

The characteristics of the chordwise variations on the pressure distributions on the lower surface are observed in the C^l_p curves for $\bar{y} = 0.2$. These curves are shown in Figs. 11 and 12 for the 60 and 75 deg deltas, respectively, at a series of angles of attack. In both wings, the C^l_p values are, in general, positive. They are largest near the apex and decrease in the downstream direction. They increase with increasing angle of attack regardless of whether the leading-edge vortices are affected by VB. Comparison of the C^l_p curves for the two wings at the same angles of attack ($\alpha = 10$, 20, and 35 deg) shows that the C^l_p values on the forward section of the 60 deg

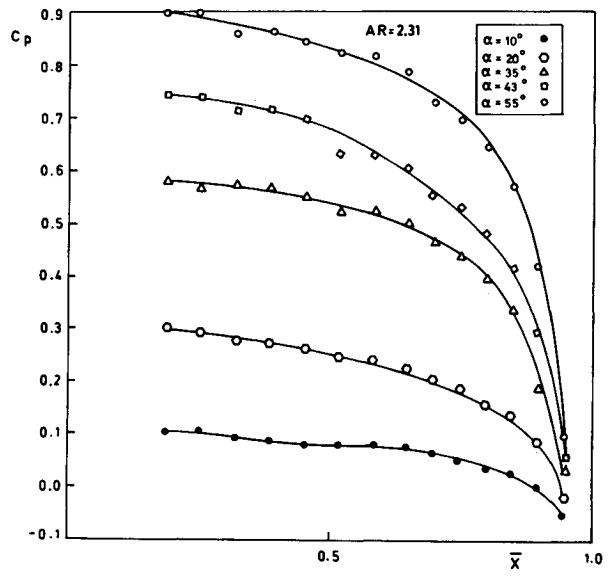

Fig. 11 Chordwise C_p^l profiles along $\bar{y} = 0.2$ on the 60 deg delta at various incidence angles.

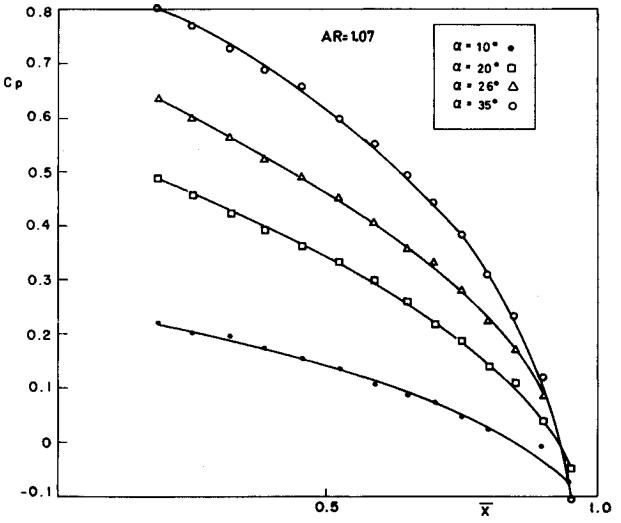

Fig. 12 Chordwise C_p^l profiles along $\bar{y} = 0.2$ on the 75 deg delta at various incidence angles.

swept wing (where the effects of the Kutta conditions are negligible) are larger than on the 75 deg swept wing. Evidently, the higher-aspect-ratio planform poses a larger obstruction to the oncoming flow to generate larger static pressures on the lower surface.

Normal Force and Pitching Moment

The coefficients of the potential and vortical components of the normal force, as defined by the leading-edge suction analogy,[11] as well as the normal force coefficient itself, are given as a function of the incidence angle in Figs. 13 and 14 for the 60 and 75 deg swept wings, respectively. These coefficients were obtained by integration of the surface pressures by using a procedure that utilizes results of the small-perturbation potential flow wing theory. This is the same theory on which the leading-edge suction analogy is based. In the above-mentioned procedure (which is outlined in detail in Refs. 8 and 12), C_{NP} (the potential contribution to C_N) is obtained from the surface pressures on the windward side where the flow is attached, and C_{NV} (the vortical contribution to C_N) is the difference between C_N and C_{NP}.

The results presented here summarize quantitatively some of the features observed in the pressure distributions. In both

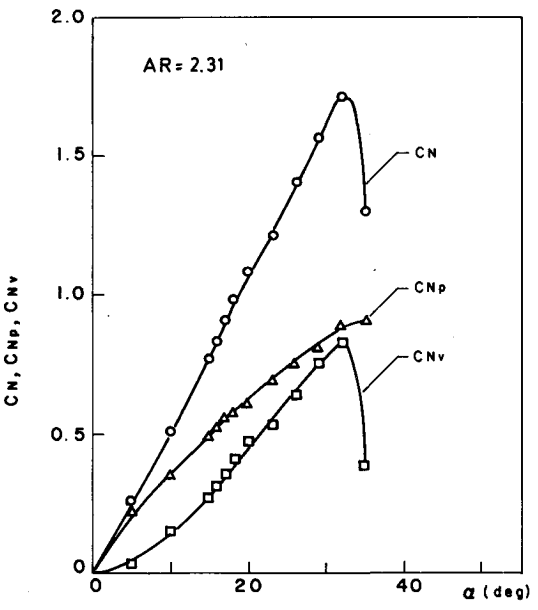

Fig. 13 Potential and vortical components and the normal force vs angle of attack for the 60 deg delta.

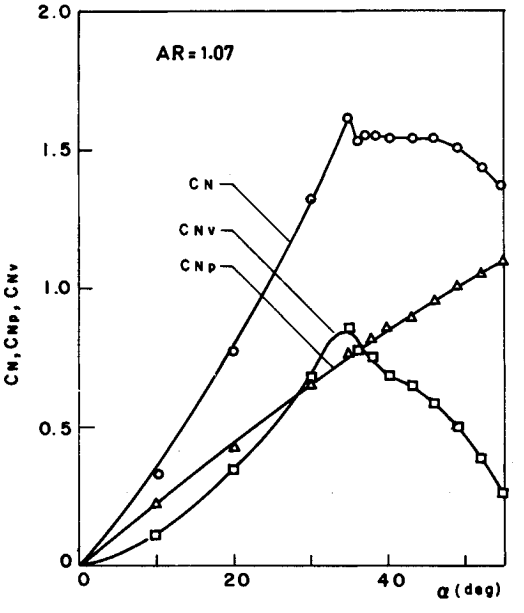

Fig. 14 Potential and vortical components and the normal force vs angle of attack for the 75 deg delta.

wings, C_{NV} increases with incidence as long as the shed vortices are not affected by VB, and its proportional contribution to C_N increases with decreasing aspect ratio. In the 60 deg delta, C_{NV} and C_N increase with incidence even when VB is present as long as it has not reached the apex region ($\alpha \leq 32$ deg). This indicates that the decrease in the derivative $\partial|C^u_{p,\min}|/\partial\alpha$ in the vortex portions affected by VB (observed in Fig. 9) is not manifested in a similar decrease in the vortex lift. Evidently, at $\alpha < 32$ deg, the increased width of the suction peaks affected by VB (and observed in the spanwise pressure distributions) compensates for the decrease in $|C^u_{p,\min}|$ to keep $\partial C_{NV}/\partial\alpha$ positive. The appearance of VB at the apex is manifested in a sharp decrease in $dC_{NV}/d\alpha$ and $dC_N/d\alpha$ from positive to negative values. In the 75 deg swept wing, a similar decrease in these derivatives is evident when the VB has reached the trailing edge ($\alpha \cong 35$ deg). The magnitude of these derivatives in the 75 deg swept delta is considerably smaller than that of the 60 deg swept wing. The C_{NP} of both wings increases with incidence regardless of the presence of

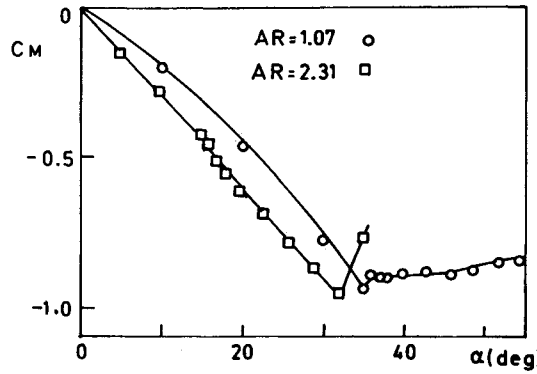

Fig. 15 Pitching moment vs angle of attack for the 60 and 75 deg deltas.

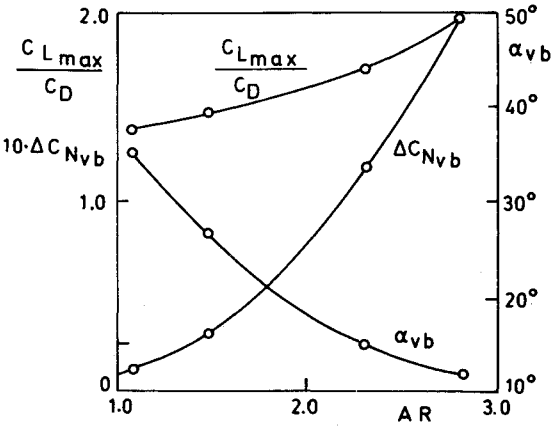

Fig. 16 Effect of aspect ratio on the incidence angle at which VB appears at the trailing edge, on the aerodynamic efficiency, and on ΔC_{Nvb}.

VB and its proportional contribution increases with increasing aspect ratio. The characteristics of C_N, the sum of C_{NV} and C_{NP}, are similar to those of C_{NV}. In particular, the incidence angles for $C_{N,\max}$ are approximately equal to the angle where C_{NV} attain their maximum value.

Figure 15 features the pitching moment coefficients for the 60 and 75 deg swept wings. This figure shows that C_M of both wings is negative and decreases with increasing incidence up to the angle of attack at which the wing stalls. At these angles, $dC_M/d\alpha$ changes from negative to positive values. The magnitude of this derivative in the poststall range is considerably smaller for the lower-aspect-ratio wing.

Figure 16 serves as a summary of the present work. It shows the influence of the aspect ratio on 1) the average lift-to-drag ratio, based on $C_{L,\max}$, 2) α_{vb}, the angle of attack at which VB appears at the trailing edge (the data are taken from Ref. 1), and 3) ΔC_{Nvb}, the maximum increase in C_N relative to $C_{N\max}$. ΔC_{Nvb} represents the ability of the VB, when it crosses the trailing edge, to reduce $dC_N/d\alpha$ and to cause lift saturation. These results indicate that this ability decreases with increasing aspect ratio or that the effect of VB on the suction induced by the vortices becomes weaker with increasing aspect ratio. The lift-to-drag ratio increases with increasing aspect ratio. For example, an increase in the aspect ratio from 1.07 to 2.8 results in an approximate 40% increase in this ratio.

References

[1]Wentz, W.H., Jr. and Kohlman, D.L., "Wind Tunnel Investigation of Vortex Breakdown on Slender Sharp-Edged Wings," NASA CR-98737, 1968.

[2]Lawford, J.A. and Beauchamph, A.R., "Low Speed Wind Tunnel Measurements on a Thin Sharp Edged Delta Wing with 70 deg Leading Edge Sweep, with Particular Reference to the Position of Leading Edge Vortex Breakdown," Aeronautical Research Council, U.K., R&M 3338, 1961.

[3]Hummel, D., "Untersuchungen uker das Aufplatzen der Wirbel an schlanken Deltaflugeln," *Zeitschrift für Flugwissenschaften,* Vol. 13, No. 5, 1965, pp. 158–168.

[4]Kirkpatrick, D.L.I., "Analysis of the Static Pressure Distribution on a Delta Wing in Subsonic Flow," Aeronautical Research Council, U.K., R&M 3619, 1968.

[5]McKernan, J.F. and Nelson, R.C., "An Investigation of the Breakdown of the Leading Edge Vortices on a Delta Wing at High Angles of Attack," AIAA Paper 83-2114, 1983.

[6]Cheremukin, G.A., Tuneva, E.A., and Piokin, E.J., "Flow Past a Small Aspect Ratio Delta Wing with Vortex Filament Breakdown," *Aviatsionnia Teckhnika,* Vol. 21, No. 4, 1968, pp. 162–167.

[7]Earnshaw, P.B. and Lawford, J.A., "Low-Speed Wind-Tunnel Experiments on a Series of Sharp-Edged Symmetrical Models," Aeronautical Research Council, U.K., R&M 3424, 1966.

[8]Zohar, Y., "The Effects of Vortex Breakdown on the Aerodynamic Properties of Delta Wings," M.Sc.Thesis, Technion—Israel Institute of Technology, Haifa, 1984.

[9]Brown, C.E. and Michael, W.H., "On Slender Delta Wings with Leading-Edge Separation," NACA TN 3430, 1950.

[10]Smith, J.H.B., "Improved Calculations of Leading-Edge Separation from Slender, Thin Delta Wings," *Proceedings of the Royal Society of London,* Ser. A, Vol. 306, 1968, pp. 67–90.

[11]Polhamous, E.C., "Predictions of Vortex-Lift Characteristics by a Leading-Edge Suction Analogy," *Journal of Aircraft,* Vol. 8, April 1971, pp. 193–199.

[12]Er-El, J. and Yitzhak, Z,. "Experimental Examination of the Leading-Edge Suction Analogy," *Journal of Aircraft*, Vol. 25, March 1988, pp. 195–199.